

Pulsed operation of a TEA CO₂ laser under the conditions of the growth of an optical inhomogeneity of the active medium at high specific pump energies

K N Makarov, V K Rerikh, Yu A Satov, A E Stepanov, S V Khomenko

Abstract. A CO₂ laser system with self-modulation of the intracavity losses was developed. This system was capable of generating efficiently pulses free of a radiation ‘tail’ typical for CO₂ lasers. A simple method was used to detect the optical inhomogeneity of the medium of a gas-discharge TEA module. The results of the measurements are presented.

1. Introduction

The profile of an output pulse of an atmospheric-pressure TEA CO₂ laser is typically of 40–200 ns duration and is followed by a slowly decaying ‘tail’ or by another pulse of low intensity and of 1–5 μs duration. The radiation-pulse characteristics depend on the pump energy of the medium, the cavity Q-factor, and the composition of the active medium. However, in regimes close to effective peak-power generation, the energy in the first peak does not exceed 30%–50% of the total pulse energy. The presence of a long radiation ‘tail’ is undesirable in many practical applications. In particular, in the generation of multicharged ions in a laser plasma a low-intensity radiation ‘tail’ not only imposes an additional optical load on the optical components, but also generates a large number of ions with a low charge and vigorously vaporises the material of the target. The use of such pulses in devices with repetitively pulsed operation may greatly reduce the operating lifetime of the laser system.

The generation of a pulse ‘tail’ may be suppressed by the use of a low-Q cavity or of nitrogen-free mixtures. However, this leads to an appreciable lowering of the specific output characteristics of the radiation and to an increase in the duration of the first radiation peak. The application of active or passive modulation [1–3] appreciably complicates the oscillator system. Among the systems listed, the most effective is one employing an electro-optical switch but having a short operating lifetime in a repetitively pulsed regime for energy densities of ~100 mJ cm⁻².

The aim of the study was to construct a CO₂ laser with self-modulation of the intracavity losses, effectively generat-

ing pulses free of the ‘tail’ typical for CO₂ lasers. An additional task which we set ourselves was the attainment of lasing based on a single longitudinal mode in order to achieve a smooth temporal output pulse profile.

In the present study, measurements were made of the optical inhomogeneities appearing in the active medium of a TEA laser after the passage of a discharge-current pulse at high specific input energies. The method is based on measurements of the gain experienced by a weak (probe) signal in the TEA module. It was observed that, for high (not greater than 200 mJ cm⁻³) specific energy inputs into the discharge, the gain exhibited an ‘anomalous’ behaviour in the course of ~0.5–1.0 μs after the appearance of the discharge current. A typically short period of the decrease in gain and the appearance of a ‘negative’ probe signal were observed, which corresponds to the appearance of additional losses in the medium (Fig. 1). This is probably the result of the deflection of the probe signal away from the photodetector window, which was confirmed by the results of studies of various optical inhomogeneities in a pulsed self-sustained discharge [4–7].

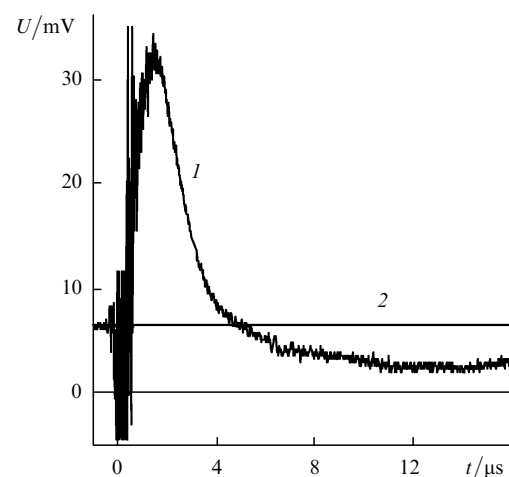


Figure 1. Typical time dependences of the amplitudes of the probe (1) and reference (2) signals.

K N Makarov, V K Rerikh, Yu A Satov, A E Stepanov, S V Khomenko
Troitsk Institute of Innovative and Thermonuclear Fusion Investigations
(State Scientific Centre of the Russian Federation), 142092 Troitsk,
Moscow province, Russia

Received 22 January 1999; revision received 28 October 1999
Kvantovaya Elektronika 30 (3) 305–309 (2000)
Translated by A K Grzybowski

The various mechanisms of the breakdown of the homogeneity of the medium reduce, in the final analysis, to a loss of homogeneity of the energy deposition in the discharge or to inhomogeneities of the radiation field. For example, volume inhomogeneities of the refractive index, arising immediately after the end of the discharge pulse, have been observed [5]. They are due to regular inhomogeneities

in the distribution of the preionisation photoelectron density and the energy-evolution inhomogeneities in the discharge volume.

The influence on the radiation of a CO₂ laser by the refractive-index inhomogeneities in the direction away from the axis to the boundary of the discharge-current profile (the lens effect) has been investigated theoretically and experimentally [4]. In the discharge TEA module examined in the present study, the possible causes of the energy-evolution inhomogeneities may be, according to the authors, both the processes described in Refs [4, 5] and the effects arising in the electrical-breakdown stage (for example, the influence of the streamer electrical-breakdown mechanisms under the conditions of high overvoltages), as well as the influence of various discharge-contraction mechanisms (in the first place, thermal instabilities).

A detailed study of the causes of the appearance of optical inhomogeneities and of local optical-density gradients is outside the scope of the present investigation in which measurements were made of the optical inhomogeneity averaged over the discharge volume and its influence, from the standpoint of the diffraction losses of a TEA CO₂ laser cavity, was estimated.

2. Experimental apparatus and methods used in the measurements

The experimental apparatus consisted of a TEA discharge module with a 17 mm × 17 mm × 450 mm active medium, an He–Ne laser ($\lambda = 0.63 \mu\text{m}$), and a photodetector with an objective (Fig. 2). A characteristic feature of the electric circuit in the discharge module was the formation of an initial peak in the voltage pulse with a steep leading edge and an amplitude appreciably exceeding (by a factor greater than two) the breakdown voltages for the N₂–CO₂–He mixtures employed [8]. The discharge was then of a stable volume character and did not go over to the spark phase over a wide (up to 300 mJ cm⁻³) range of input energies in the presence of a content of molecular gases up to 80%.

The cw radiation from an He–Ne laser passed through the probe section of the medium of the gas-discharge module and was directed into an objective (3) with the focal length $F = 200 \text{ mm}$, which focused the radiation into a photodiode detector (4). In order to match the size of the photodiode (600 $\mu\text{m} \times 600 \mu\text{m}$) to the beam diameter, the detector was placed at the corresponding point in a geometrically converging beam, as shown in Fig. 2. The measuring system detected the change in the illumination of the detector with a temporal resolution of $\sim 100 \text{ ns}$. A modulator in the form of a rotating disk with openings was used to calibrate the maximum signal (the signal corresponding to 100% losses) in the system. The linearity of the detector in the dynamic range of the signals

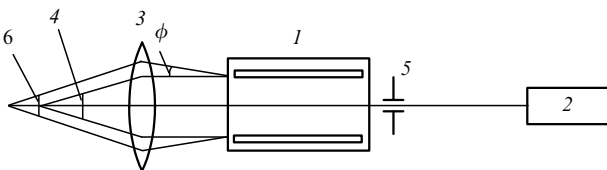


Figure 2. Experimental setup: (1) TEA module; (2) He–Ne laser; (3) objective; (4) photodetector; (5) aperture; (6) scattering circle, diameter, $2\phi F$.

employed was tested with the aid of optical filters of known density. The voltage pulse over the discharge gap of the TEA module was measured with the aid of a 5 k Ω resistance detector, the current in which was recorded with a Rogowski loop. The laser-pulse profile, illustrated in Fig. 1, was recorded by a photodetector having a temporal resolution not greater than 1 ns. All the oscillograms presented in this communication were recorded with the aid of a two-channel LeCroy oscilloscope, which digitised the signal in steps of 2.5 ns and had an amplifier with a band 400 MHz wide.

3. Results of measurements and their analysis

Fig. 3 presents a series of oscillograms demonstrating the method of measurement in relation to the probing of the gas discharge in a N₂:He = 1:1 mixture ($p = 1 \text{ bar}$). An He–Ne laser beam having a diameter $d = 1.5 \text{ mm}$ was passed through various regions of the discharge volume near the central plane crossing the electrodes. The instant $t = 0$ coincides with the beginning of the discharge-current pulse, a zero signal indicating a constant initial illumination of the photodiode. The growth of the signal at the beginning of the oscillograms reflects the additional illumination of the detector by the radiation of the discharge in the TEA module and the subsequent decrease in illumination is induced by the appearance of various losses in the medium investigated. The signal corresponding to the total absence of the probe-beam radiation was in this case $\sim 70 \text{ mV}$. The measurements showed that, when the specific energy input in the discharge

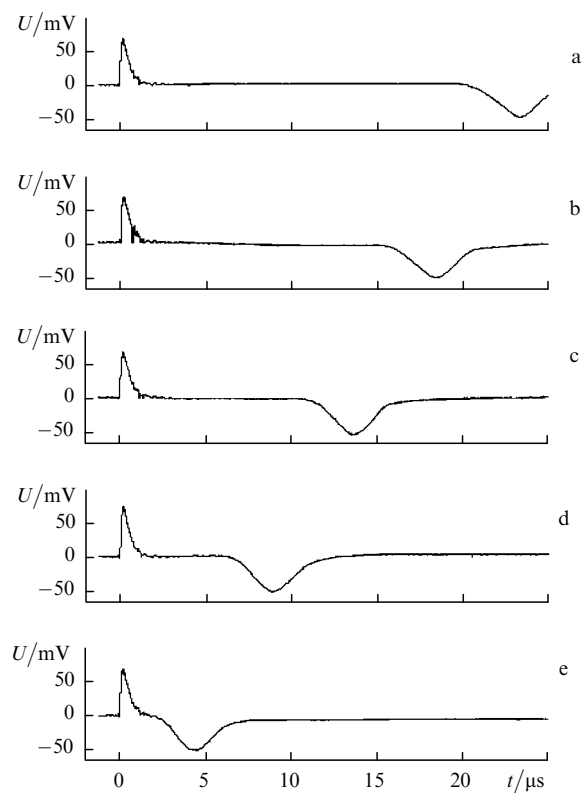


Figure 3. Time dependences of the photodetector signal on displacement of the probe beam from the electrodes: $s = +6 \text{ mm}$ (a); $s = +3 \text{ mm}$ (b); $s = 0$ (c); $s = -3 \text{ mm}$ (d); $s = -6 \text{ mm}$ (e); the beam was displaced from the central plane through the module in the positive (towards and anode) and negative (towards the cathode) directions.

is 100 mJ cm^{-2} , the dominant medium-perturbation factor is the well-known shock wave propagating from the cathode to the anode. The oscillograms presented make it possible, in particular, to discover that the rate of propagation of the shock wave was $7 \times 10^4 \text{ cm s}^{-1}$.

Fig. 4 presents similar data on the probing of the paraxial region of the discharge in the $\text{CO}_2 : \text{N}_2 : \text{He} = 4 : 1 : 5$ mixture for different specific input energies. A shock wave propagating from the cathode to the anode, the velocity of which increased with increasing input energy, was observed in these experiments. Under these conditions, a characteristic effect is the appearance of volume losses in the active medium, an appreciable increase of which occurs already at the end of the discharge-current pulse (with a delay of $\sim 0.6\text{--}0.7 \mu\text{s}$) and is independent of the probed region within the limits of the sensitivity of the method.

The optical inhomogeneity averaged over the volume of the active medium was measured with the aid of an He–Ne laser beam expanded to a diameter $d = 10 \text{ mm}$ and transmitted along the axis of the interelectrode gap. The results of the measurements are presented in Fig. 5. The background illumination of the detector by the discharge was minimised by optical filters with a transmission band in the red part of the spectrum.

The analysis of the experimental data was based on the fact that the disappearance of the signal on the photodetector was the result of the refraction of the radiation in the gas discharge on local optical inhomogeneities associated with the occurrence of inhomogeneous energy evolution and hence with the inhomogeneity of the density and temperature. The change in the optical inhomogeneity averaged over the volume, which can be described by an effective optical-density gradient, was recorded in the experiment. For small

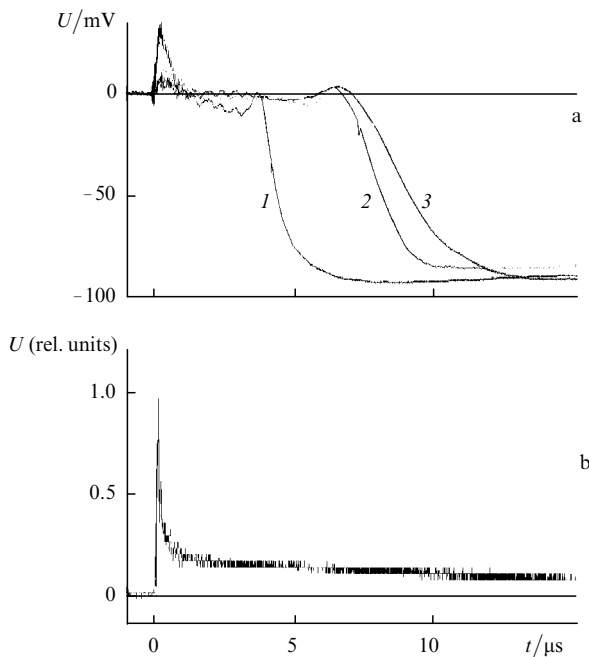


Figure 4. Time dependence of the photodetector signal for the initial position of the probe beam, 1.5 mm in diameter, on the discharge axis, the pressures of the mixture $p = 1 \text{ bar}$ (1, 2) and 0.6 bar (3), and the specific input energies $W = 300 \text{ mJ cm}^{-3}$ (1), 100 mJ cm^{-3} (2), and 60 mJ cm^{-3} (3) (a) and time dependence of the temporal profile of an out-pulse (b).

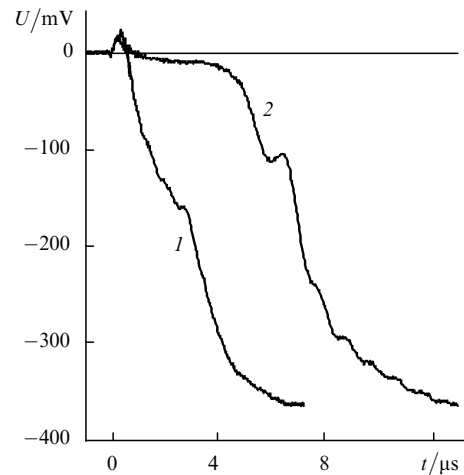


Figure 5. Time dependences of the photodetector signals for $W = 100 \text{ mJ cm}^{-3}$ (1) and 300 mJ cm^{-3} (2). Probe beam diameter was 10 mm.

deflection angles ϕ , one may write

$$\phi = \frac{1}{n} \frac{dn}{dr} l, \quad (1)$$

where n is the refractive index; dn/dr is the transverse optical-density gradient; l is the length of the medium.

As can be seen from simple geometrical considerations (Fig. 2), the photodiode signal $U(t)$, normalised with respect to unity, is linked to the ‘scattering circle’ area $\pi(\phi F)^2$ by the relationship

$$U(t) = \frac{d_0^2}{\pi(\phi F)^2 + d_0^2}, \quad (2)$$

where d_0 is the size of the square entry window.

The time dependence of the angle of refraction ($\lambda = 0.63 \mu\text{m}$), calculated by formula (1), and the corresponding photodiode signal $U(t)$ are shown in Fig. 6. These results refer to a discharge in the $\text{CO}_2 : \text{N}_2 : \text{He} = 1 : 1 : 5$ mixture with a specific input energy of $\sim 250 \text{ mJ cm}^{-3}$. Evidently, $1 \mu\text{s}$ after the start of the current pulse the inhomogeneity of the

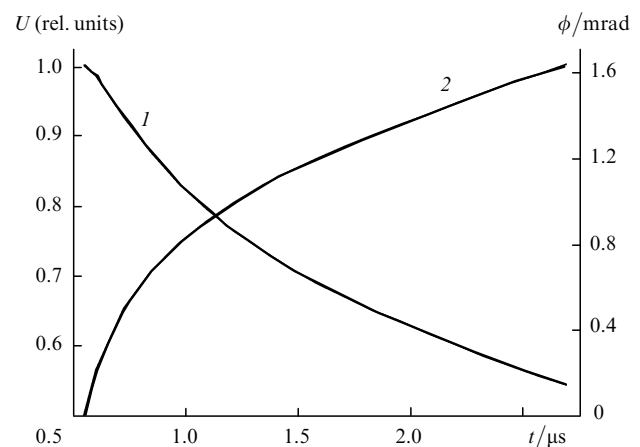


Figure 6. Time dependence of the refraction angle ϕ ($\lambda = 0.63 \mu\text{m}$) calculated by formula (1) (1) and the corresponding photodiode signal U (2).

medium is such that it can be described by an effective refraction coefficient of ~ 0.9 mrad and the corresponding density gradient $(1/\rho)(d\rho/dx) = 2 \times 10^{-5} \text{ cm}^{-1}$.

The influence of molecular refraction on radiation with $\lambda = 10.6 \text{ }\mu\text{m}$ can be estimated by means of the familiar Cauchy dispersion formula:

$$n - 1 = A_1(1 + B_1/\lambda^2).$$

Since the coefficient A_1 and B_1 for various gases differ little, it is possible to employ the tabulated data for air: $A_1 = 28.8 \times 10^{-5}$, $B_1 = 5.7 \times 10^{-9} \text{ cm}^2$. Evidently, the optical inhomogeneity in air is 2.4 times smaller than in the active medium of the CO_2 laser, but it reaches a value corresponding to a refraction angle of ~ 0.3 mrad $1 \text{ }\mu\text{s}$ after the start of the discharge-current pulse. Such inhomogeneities may explain the absence of a pulse generation 'tail', because they are comparable with the diffraction-limited divergence of the probe beam.

4. Temporal and energy characteristics of a TEA CO_2 laser

The infringements of the homogeneity of the active medium for a CO_2 laser described in the previous section are in most practical cases negligible, but for certain laser parameters they may influence the temporal characteristic of a CO_2 laser operating in the free-running regime. Such parameters are evidently the input energy and the gas composition of the active mixture, which must be selected from the standpoint of effective lasing in the first peak with a minimal residual 'tail'. It is well known [11] that this mixture composition is close to $\text{CO}_2 : \text{N}_2 : \text{He} = 4 : 1 : 5$. In addition, it is necessary to optimise the Q-factor of the cavity and its length in order to ensure an appreciable delay of the onset of lasing relative to the pump current. The cavity configuration must be chosen to ensure the least divergence of the fundamental transverse mode.

The calculations performed to estimate the effect investigated in the case of a semiconfocal cavity 2.75 m long and having an aperture diameter in the beam waist of 8 mm (Fresnel number $N = 0.55$) have shown that the initial diffraction losses, amounting to 5%, reach 50% for the fundamental transverse mode $1 \text{ }\mu\text{s}$ after the start of the discharge-current pulse. Data taken from Ref. [12] were used in the calculation. The estimates permit the hope for the suppression of lasing in a TEA laser after the first pulse peak has been emitted.

The estimates obtained were tested experimentally in a hybrid CO_2 -laser system operating on the basis of the fundamental transverse and single longitudinal modes. The oscillator consisted of the TEA module described above and a low-pressure discharge tube ($p = 4$ Torr, $\text{CO}_2 : \text{N}_2 : \text{He} = 1 : 1 : 8$ mixture) with an active length of 40 cm. The cavity, 1.7 m long, was formed by a spherical copper mirror with the radius of curvature $R = -6$ m and a flat ZnSe plate anti-reflection-coated on one side to transmit at $\lambda = 10.6 \text{ }\mu\text{m}$ (the transparency was $T = 83\%$). An intracavity aperture 9 mm in diameter was placed near the plane mirror. The temporal profile of the output pulse was recorded for different energy inputs into the discharge. It was observed that, for a specific input energy exceeding 250 mJ cm^{-2} , the generation of the pulse 'tail' was suppressed with 100% reliability. Typical radiation-pulse profiles, illustrating the qualitative change in the nature of lasing, are presented in Fig. 7.

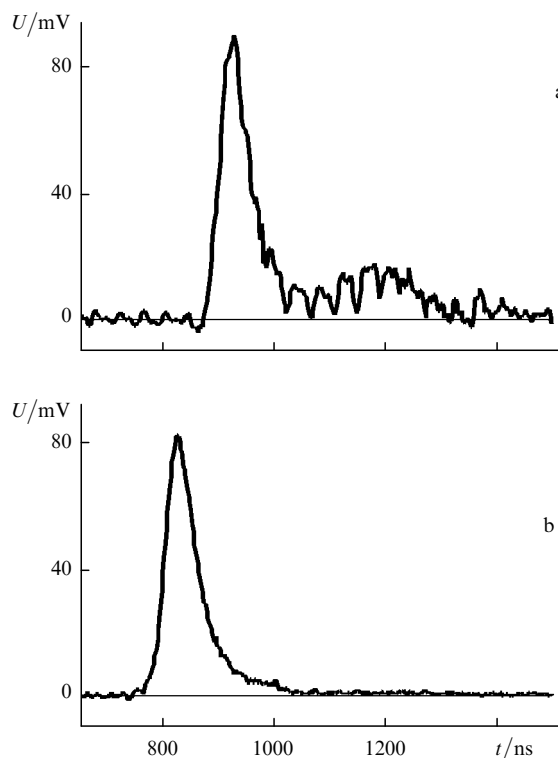


Figure 7. Typical lasing pulse profiles for small (a) and large (b) input energies.

It is noteworthy that the intracavity-losses modulation effect considered did not affect the stability of the characteristics of the first lasing peak. A master oscillator for a laser ion source was constructed at CERN on the basis of the TEA CO_2 laser prototype described in this communication [13]. The oscillator operates in a single-frequency single-mode regime with an output energy up to 200 mJ for a pulse duration of 65–70 ns and with the total absence of a radiation 'tail'. It must be stressed that the oscillator, with self-adjustment of the cavity length, is stable to within 2% in respect of the power amplitude. The spatial distribution of the radiation in the far-field zone is close to a Gaussian profile.

5. Conclusions

The parameters of a TEA CO_2 oscillator were optimised in the present study. The optimisation makes it possible to generate effectively pulses consisting of a single smooth radiation peak. The effective suppression of the pulse-generation 'tail' is attributed to the growth of an optical inhomogeneity in the active medium. The infringement of the optical homogeneity of the medium of a self-sustained gas discharge detected in the present study has been confirmed by measurements by other investigators using methods differing from ours.

Acknowledgements. The authors thank D D Malyuta and A P Napartovich for valuable discussions and also S M Savin for providing the photodetector for the experiments.

References

1. Borisov V M, Satov Yu A, Sudakov V V Prib. Tekh. Eksp. (1) 201 (1977)
2. Carlson R L, Carpenter J P, Casperson D E, et al. IEEE Quantum Electron. **QE-17** 1662 (1981)
3. Mathieu P, Otis G Proc. SPIE Int. Soc. Opt. Eng. **663** 74 (1986)
4. Verreault M, Tremblay R Can. J. Phys. **55** 1289 (1977)
5. Burtsev V A, Zelenov L A, Kamarin I L, et al. Kvantovaya Elektron. (Moscow) **15** 167 (1988) [Sov. J. Quantum Electron. **18** 107 (1988)]
6. Dimakov S A, Malakhov L N, Sherstobitov V E, Yashukov V P Kvantovaya Elektron. (Moscow) **10** 397 (1983) [Sov. J. Quantum Electron. **13** 221 (1983)]
7. Kovalev I O, Koroblev A V, Kuzmin G P, Prokhorov A M, Toker G R Pis'ma Zh. Tekh. Fiz. **15** (9) 17 (1989) [Sov. Tech. Phys. Lett. **15** 336 (1989)]
8. Satov Yu A, Smakovskii Yu B, Khomenko S V, Russian Federation Patent No. 2096881 (appl. 29 April 1996)
9. Hauf W, Grigull U Opticheskie Metody v Teplofizike (Spravochnik) [Optical Methods in Thermophysics (Handbook)] (Moscow: 1973)
10. Born M, Wolf E Principles of Optics 4th edition (Oxford: Pergamon Press, 1970)
11. Adamovich V A, Baranov V Yu, Smakovskii Yu B, Strel'tsov A P Kvantovaya Elektron. (Moscow) **5** 918 (1978) [Sov. J. Quantum Electron. **8** 526 (1978)]
12. Mikaelyan A L, Ter-Mikaelyan M L, Turkov Yu G Opticheskie Kvantovye Generatory (Lasers) (Moscow: Sov. Radio, 1967), p. 136
13. Master-Oscillator for LIS home page: <http://cliswww.cern.ch/home.html>